SRG operator evolution

A. J. Tropiano¹, S. K. Bogner², R. J. Furnstahl¹

¹Department of Physics, The Ohio State University, Columbus, OH 43210, USA
²National Superconducting Cyclotron Laboratory and Department of Physics and Astronomy,
Michigan State University, East Lansing, MI 48824, USA

(Dated: June 3, 2019)

Abstract

Brief description of project.

CONTENTS

I. Introduction	3
II. Mathematical/computational details	3
A. Building SRG unitary transformations	3
B. Momentum projection operator: $a_q^{\dagger} a_q$	3
C. Momentum distribution function: $\phi^2(k)$	4
III. Results	4
A. Entem-Machleidt N³LO non-local potential	4
B. RKE N^3LO and N^4LO semi-local potentials	8
C. Gezerlis N^2LO local potentials	13
References	16

I. INTRODUCTION

Results on SRG-evolved operators from several NN potentials.

- How operators evolve from band- and block-diagonal SRG transformations.
- Operator evolution for different potentials (regulators, chiral order, etc.)

II. MATHEMATICAL/COMPUTATIONAL DETAILS

A. Building SRG unitary transformations

Diagonalize initial and evolved Hamiltonians which we will call H(0) and H(s), respectively. This gives $\psi_{\alpha}(0)$ and $\psi_{\alpha}(s)$ for each eigenvalue indexed by α . Then the SRG unitary transformation can be computed by taking a sum over outer products of the evolved and initial wave functions:

$$U(s) = \sum_{\alpha=1}^{N} |\psi_{\alpha}(s)\rangle \langle \psi_{\alpha}(0)|, \qquad (1)$$

where N is the dimension of the Hamiltonian matrix. Here the weights are factored into the wave functions, thus U(s) is unitless.

To evolve operators, we simply apply U(s):

$$O(s) = U(s)O(0)U^{\dagger}(s), \tag{2}$$

where O(0) is the bare operator.

B. Momentum projection operator: $a_q^{\dagger}a_q$

Applying $a_q^{\dagger}a_q$ to a wave function $\psi(k)$ returns $\psi(q)$. For the discrete case, $\psi(k_i)$ is an $N \times 1$ vector and $a_q^{\dagger}a_q(k_i, k_j)$ is an $N \times N$ matrix where i, j = 1, ..., N. Then $a_q^{\dagger}a_q$ acting on $\psi(k)$ is a matrix multiplication, implying a continuous integration over d^3k . Therefore, we include a factor of $1/(k^2dk) \implies 1/(k_ik_j\sqrt{w_iw_j})$ in $a_q^{\dagger}a_q(k_i, k_j)$ where w represents the momentum weights. In matrix form,

$$a_q^{\dagger} a_q(k_i, k_j) = \frac{\delta_{k_i q} \delta_{k_j q}}{k_i k_j \sqrt{w_i w_j}},\tag{3}$$

which has units fm³. To evolve operators, we apply U(s) at this point. For mesh-independent figures, we must divide by an additional factor of $k_i k_j \sqrt{w_i w_j}$.

C. Momentum distribution function: $\phi^2(k)$

We diagonalize the Hamiltonian for eigenvectors ψ_{α} . In the 3S_1 - 3D_1 coupled channel, the S-component is given by $\psi_{\alpha}[:N]$ and the D-component by $\psi_{\alpha}[N:]$ where N is the length of the momentum mesh. Then the momentum distribution of the state α is given by,

$$|\phi_{\alpha}(k)|^{2} = |\psi_{\alpha}[:N]|^{2} + |\psi_{\alpha}[N:]|^{2}.$$
(4)

This satisfies the normalization condition $\sum_{i=1}^{N} |\phi(k_i)|^2 = 1$, implying that the factor $k^2 dk$ (or in the discrete case, $k_i^2 w_i$) is factored into the wave function. For mesh-independent figures, divide by $k_i^2 w_i$.

III. RESULTS

Organize this according to the figures. Format should be description of the calculation (previous section), followed by the figure, followed by takeaways.

A. Entem-Machleidt N³LO non-local potential

Non-local potential from [1].

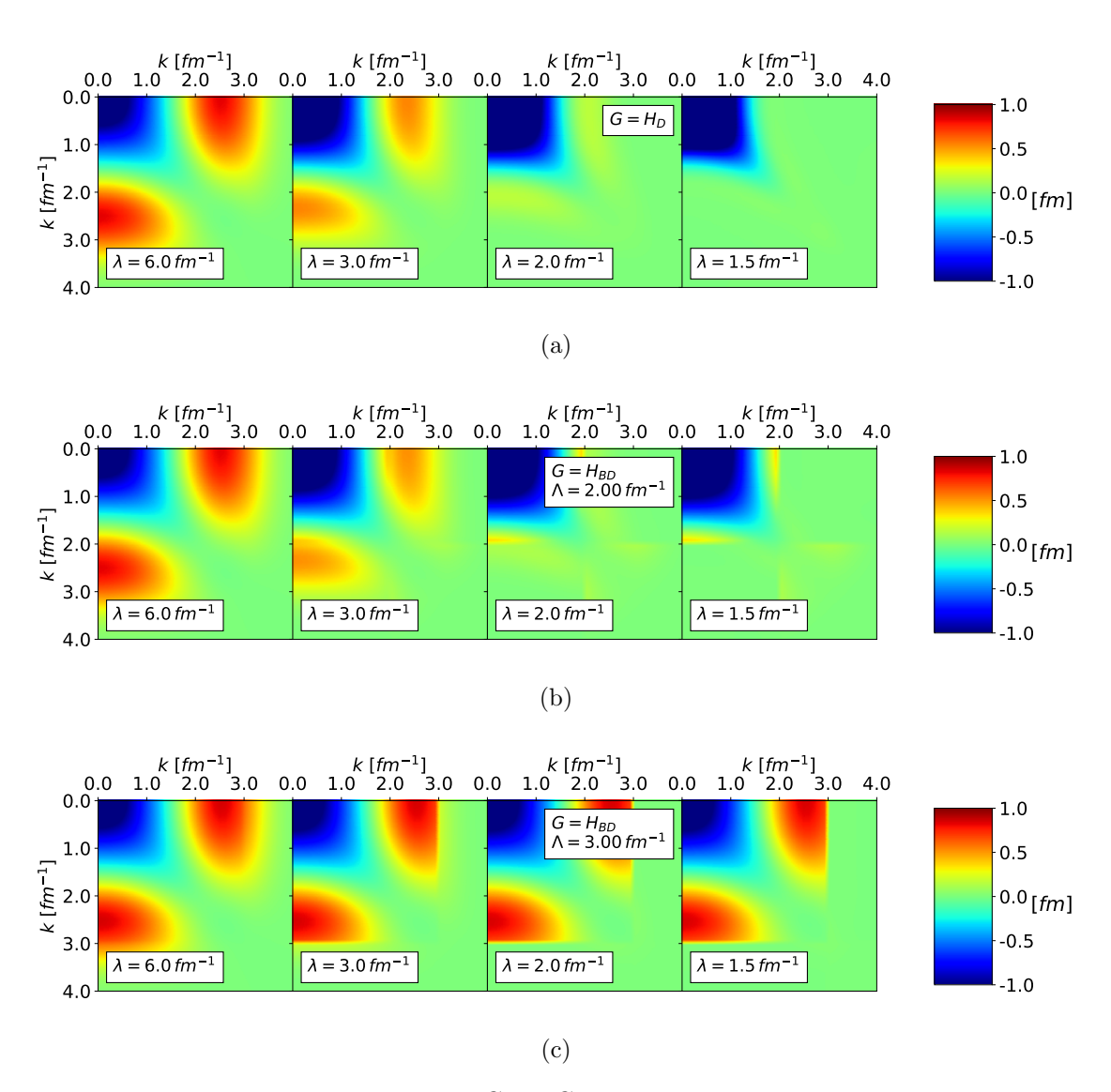


FIG. 1: Caption.

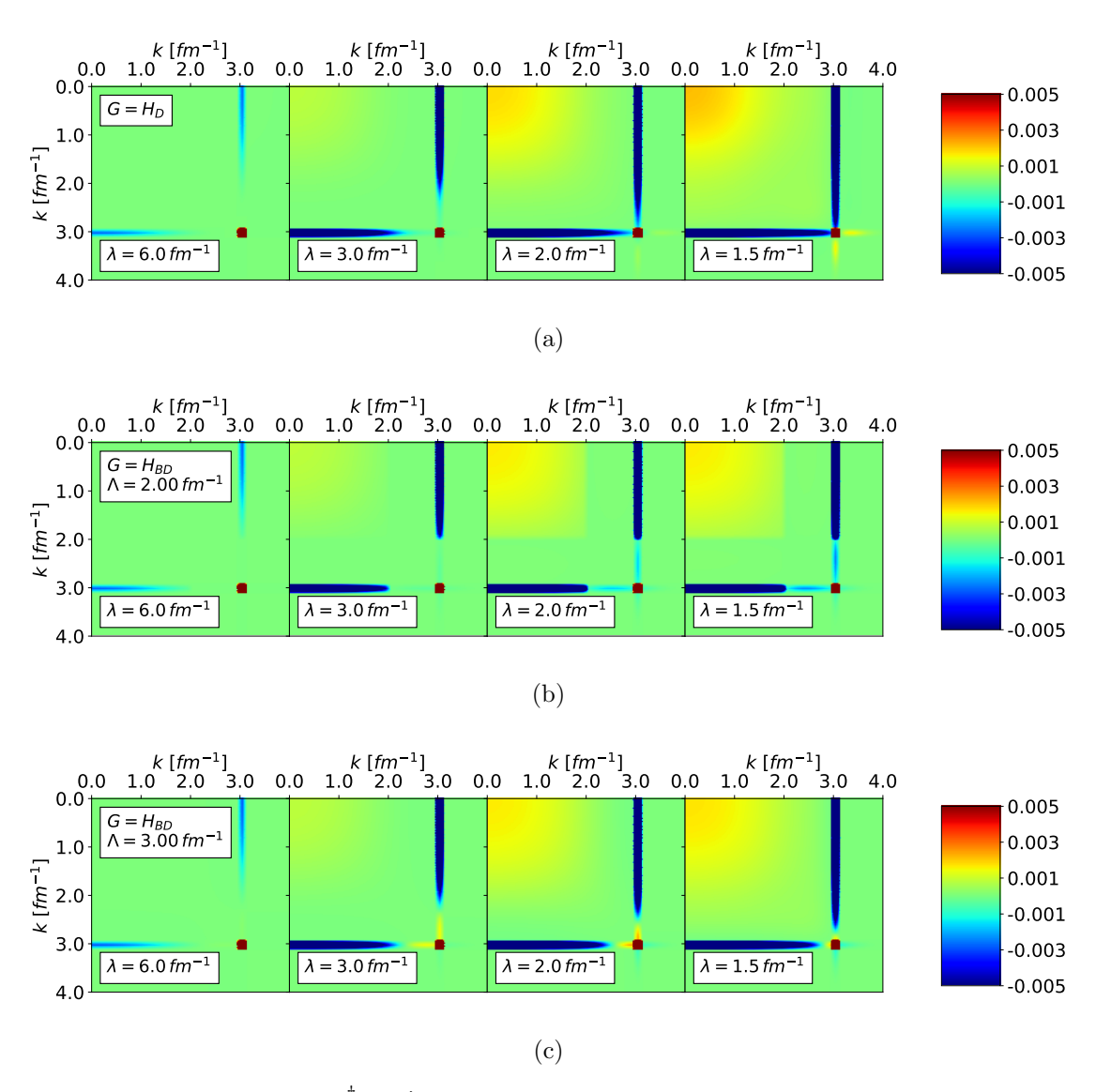


FIG. 2: Matrix elements of $\langle k|a_q^{\dagger}a_q|k'\rangle$ SRG-evolving in λ right to left under transformations from the Entem-Machleidt N³LO non-local potential with the Wegner generator (a) and block-diagonal generators decoupling at $\Lambda=2$ and 3 fm⁻¹ (b and c). Here q=3 fm⁻¹.

- The top row of Fig. 2 should match the top row in Fig. 4 of [2]. - Smeared delta function comment. - Compared block-diagonal to Wegner. - Another note about block-diagonal.

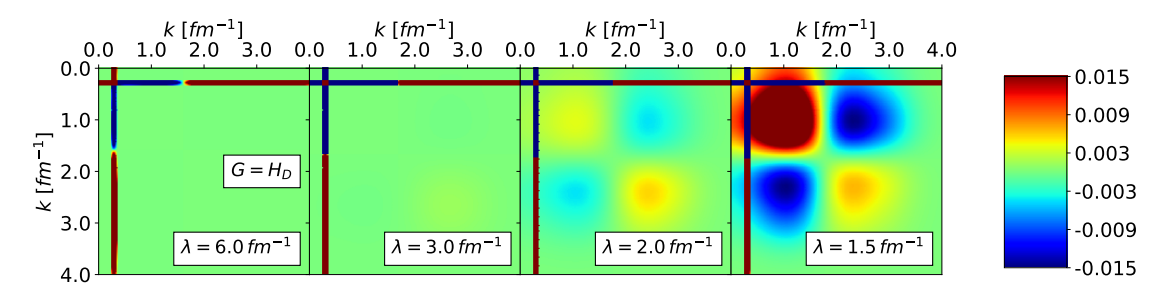


FIG. 3: Matrix elements of $\langle k|a_q^{\dagger}a_q|k'\rangle$ SRG-evolving in λ right to left under transformations from the Entem-Machleidt N³LO non-local potential with the Wegner generator. Here q=0.3 fm⁻¹.

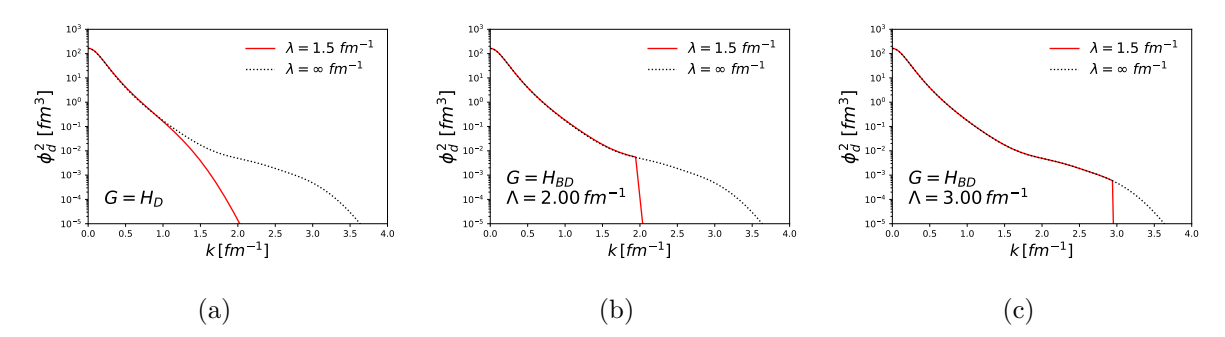


FIG. 4: Momentum probability densities of the deuteron SRG-evolving the wave function to $\lambda = 1.5$ fm⁻¹ from the Entem-Machleidt N³LO non-local potential with the Wegner generator (a) and block-diagonal generators decoupling at $\Lambda = 2$ and 3 fm⁻¹ (b and c). The black dotted line corresponds to the momentum probability density of the initial deuteron wave function.

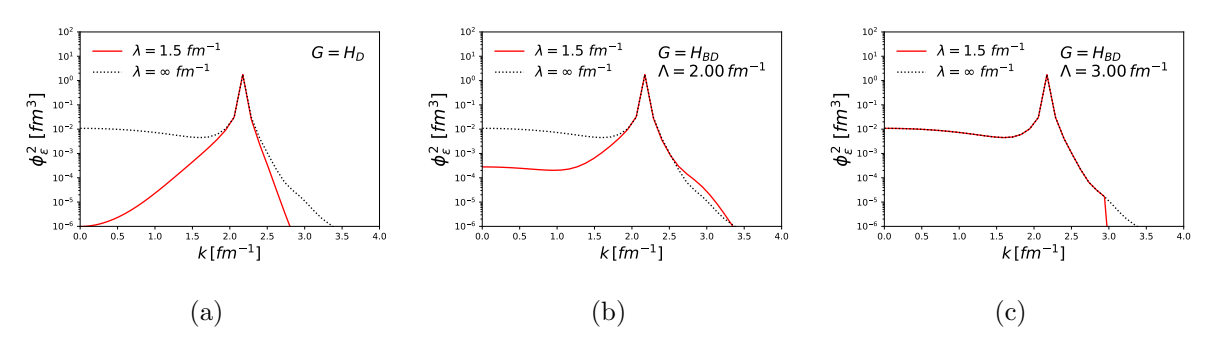


FIG. 5: Momentum probability densities of the continuum state at $\epsilon \approx 200$ MeV SRG-evolving the wave function to $\lambda = 1.5$ fm⁻¹ from the Entem-Machleidt N³LO non-local potential with the Wegner generator (a) and block-diagonal generators decoupling at $\Lambda = 2$ and 3 fm⁻¹ (b and c). The black dotted line corresponds to the initial momentum probability density.

B. RKE N³LO and N⁴LO semi-local potentials

Add takeaways for these figures. Semi-local potentials from [3].

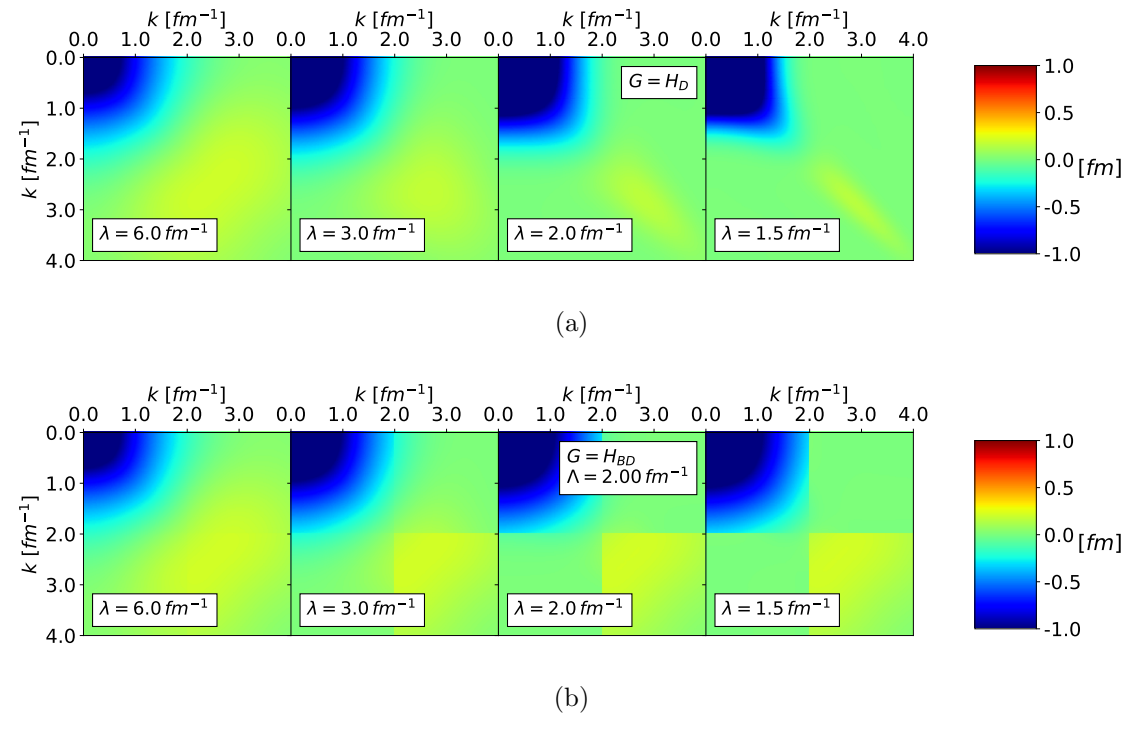


FIG. 6: Caption.

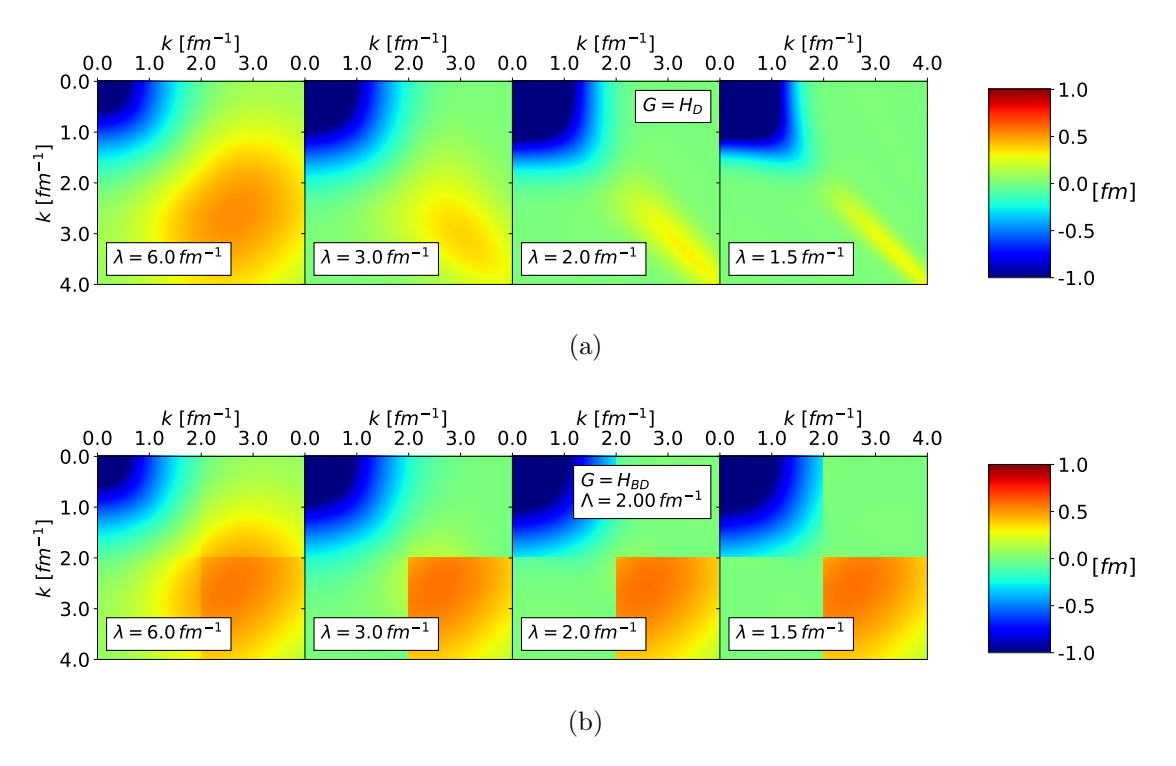


FIG. 7: Caption.

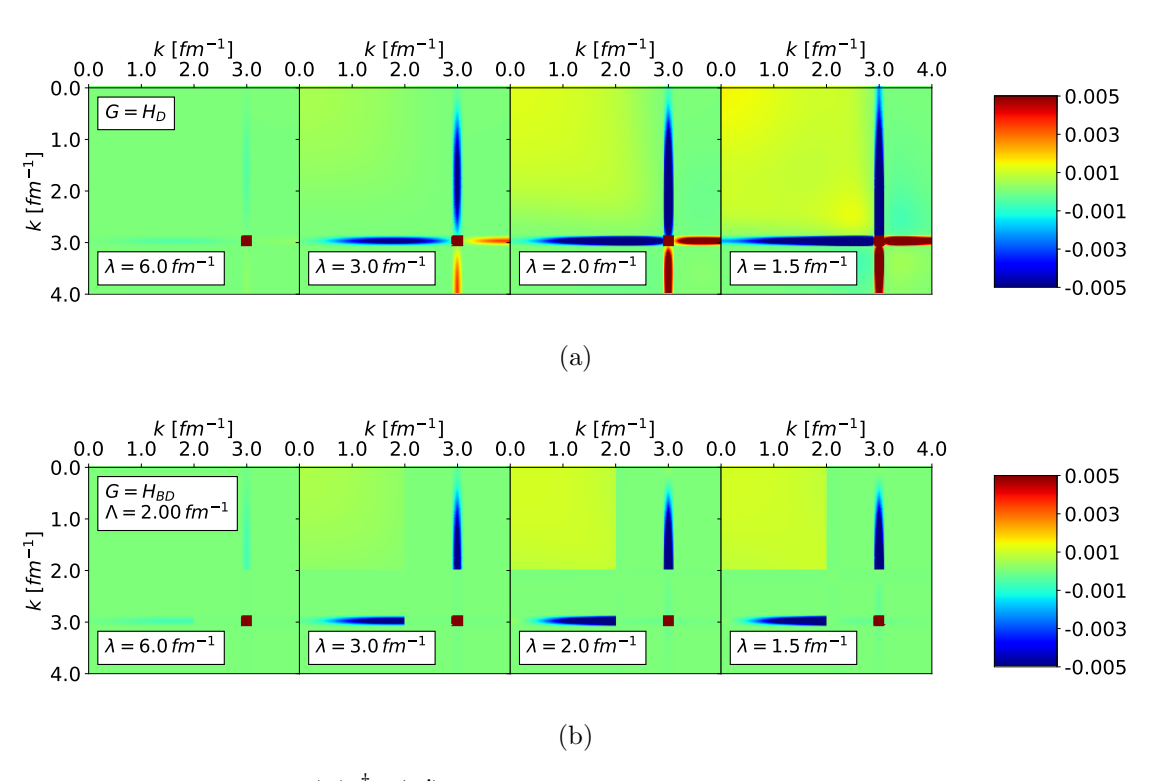


FIG. 8: Matrix elements of $\langle k|a_q^{\dagger}a_q|k'\rangle$ SRG-evolving in λ right to left under transformations from the RKE N³LO semi-local potential with the Wegner generator (a) and block-diagonal generator decoupling at $\Lambda=2~{\rm fm^{-1}}$ (b). Here $q=3~{\rm fm^{-1}}$ and the EFT cutoff is 450 MeV.

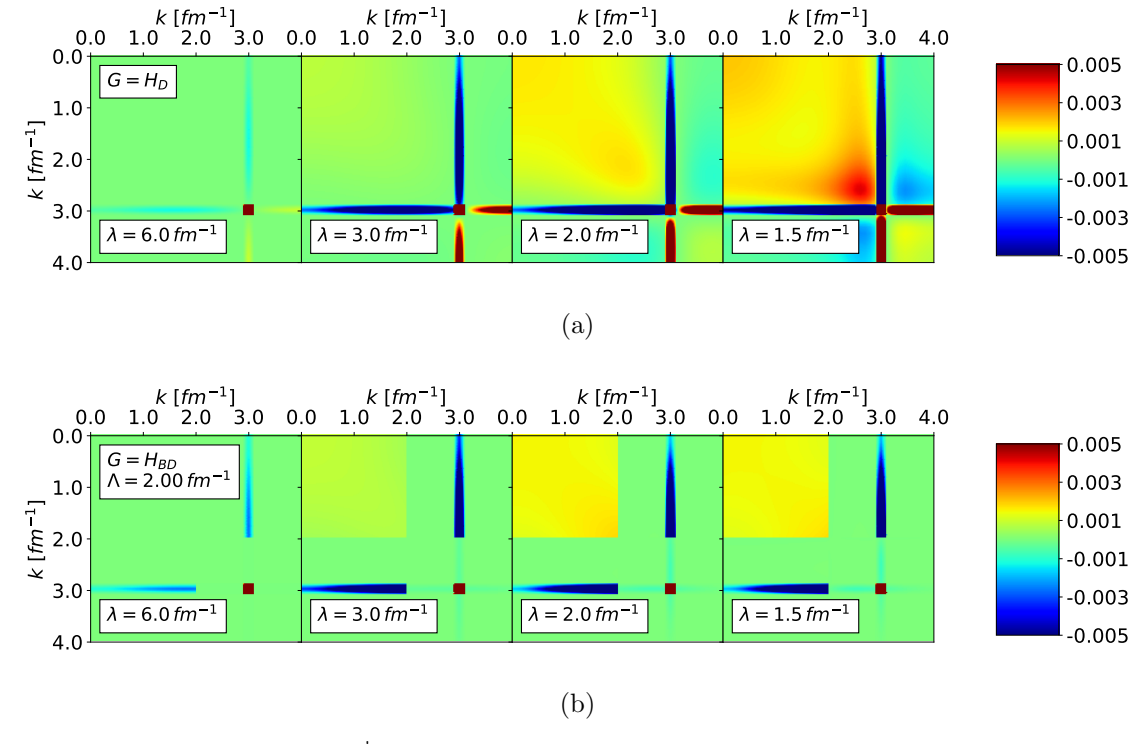


FIG. 9: Matrix elements of $\langle k|a_q^{\dagger}a_q|k'\rangle$ SRG-evolving in λ right to left under transformations from the RKE N³LO semi-local potential with the Wegner generator (a) and block-diagonal generator decoupling at $\Lambda = 2 \text{ fm}^{-1}$ (b). Here $q = 3 \text{ fm}^{-1}$ and the EFT cutoff is 500 MeV.

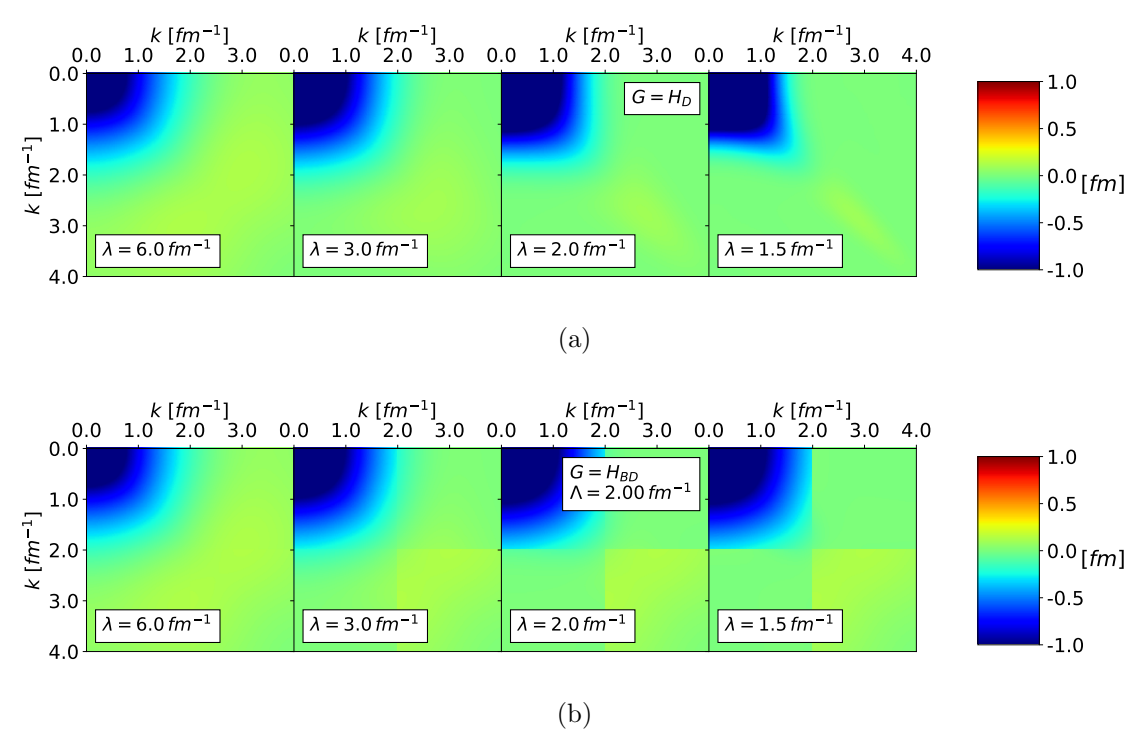


FIG. 10: Caption.

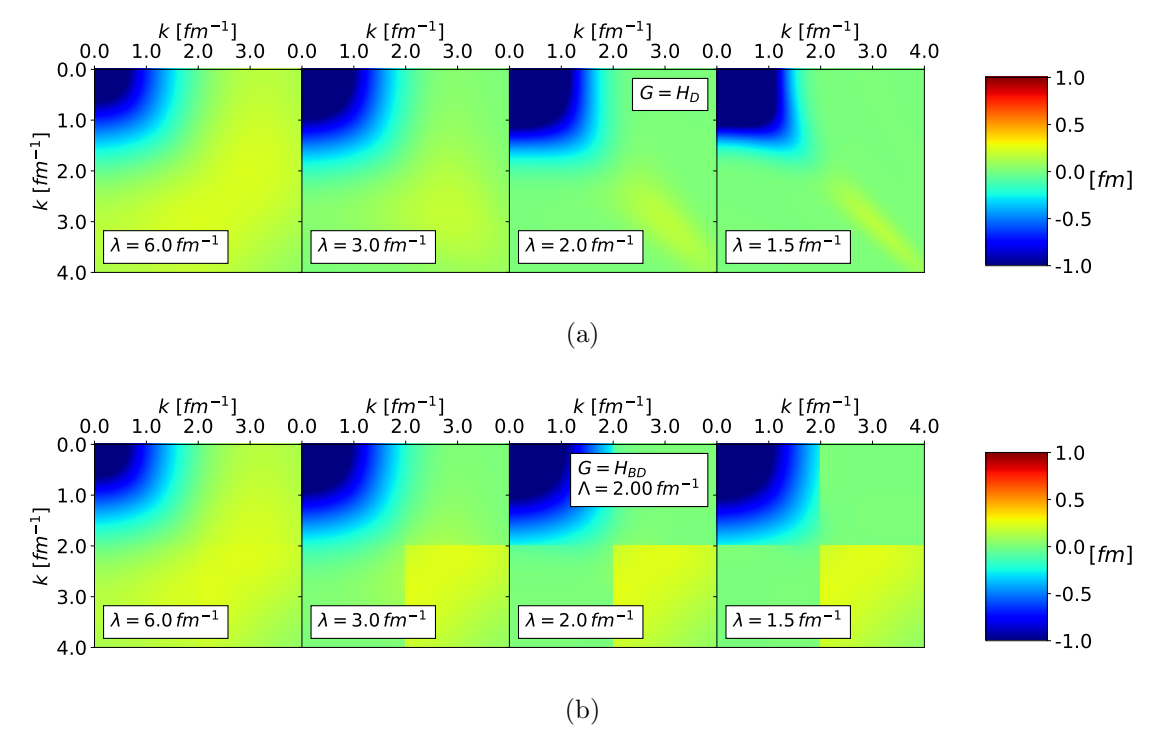


FIG. 11: Caption.

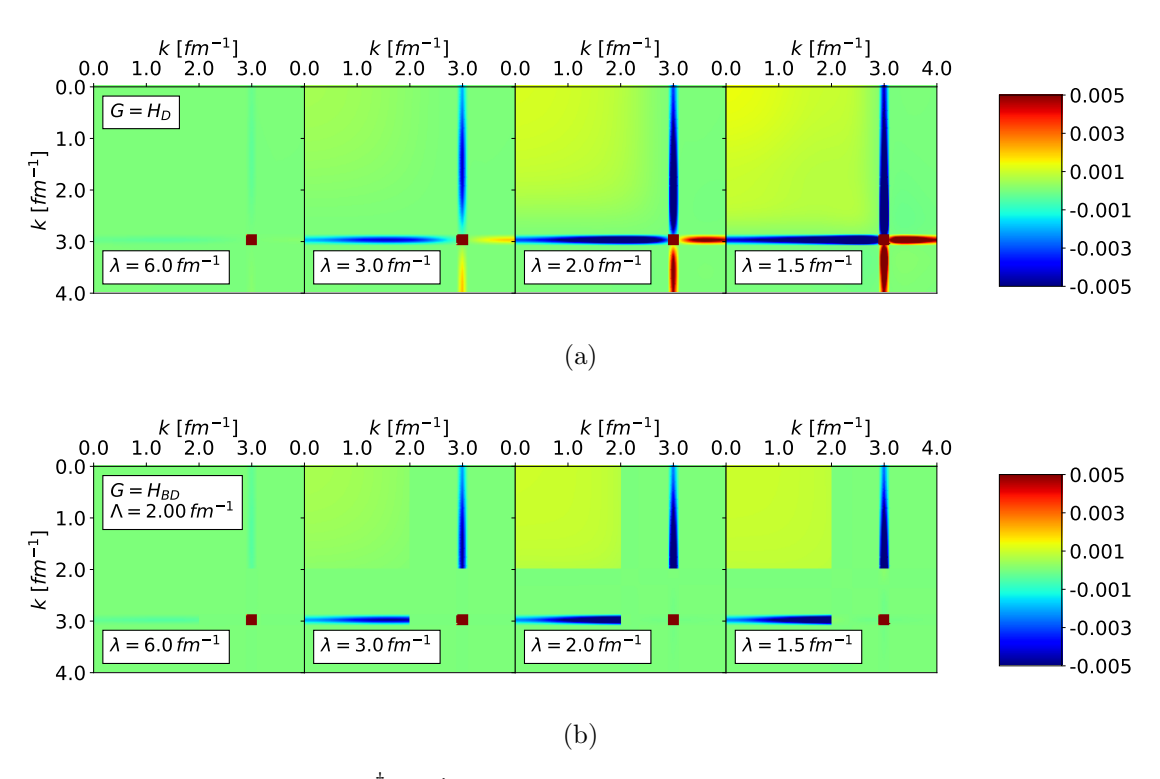


FIG. 12: Matrix elements of $\langle k|a_q^{\dagger}a_q|k'\rangle$ SRG-evolving in λ right to left under transformations from the RKE N⁴LO semi-local potential with the Wegner generator (a) and block-diagonal generator decoupling at $\Lambda=2~{\rm fm^{-1}}$ (b). Here $q=3~{\rm fm^{-1}}$ and the EFT cutoff is 450 MeV.

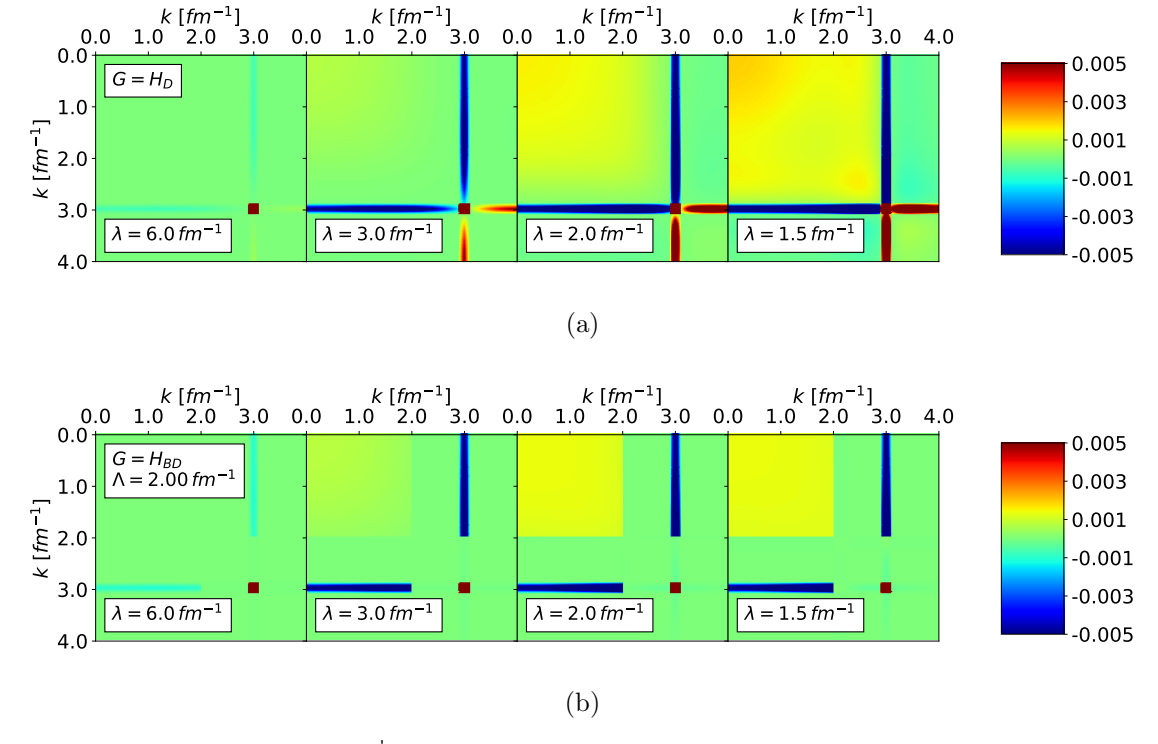


FIG. 13: Matrix elements of $\langle k|a_q^{\dagger}a_q|k'\rangle$ SRG-evolving in λ right to left under transformations from the RKE N⁴LO semi-local potential with the Wegner generator (a) and block-diagonal generator decoupling at $\Lambda=2~{\rm fm^{-1}}$ (b). Here $q=3~{\rm fm^{-1}}$ and the EFT cutoff is 500 MeV.

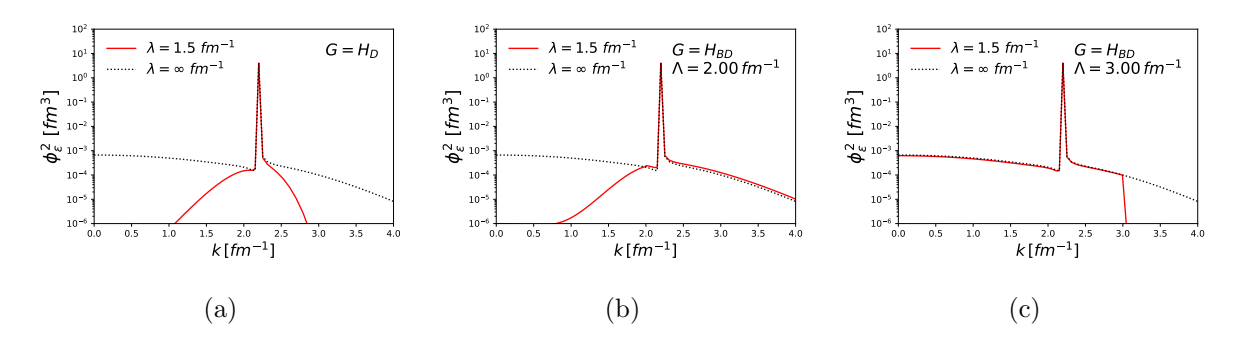


FIG. 14: Momentum probability densities of the continuum state at $\epsilon \approx 200$ MeV SRG-evolving the wave function to $\lambda = 1.5$ fm⁻¹ from the RKE N⁴LO semi-local potential with the Wegner generator (a) and block-diagonal generators decoupling at $\Lambda = 2$ and 3 fm⁻¹ (b and c). The black dotted line corresponds to the initial momentum probability density. Here the EFT cutoff is 450 MeV.

C. Gezerlis N²LO local potentials

Add takeaways for these figures. Local potentials from [4].

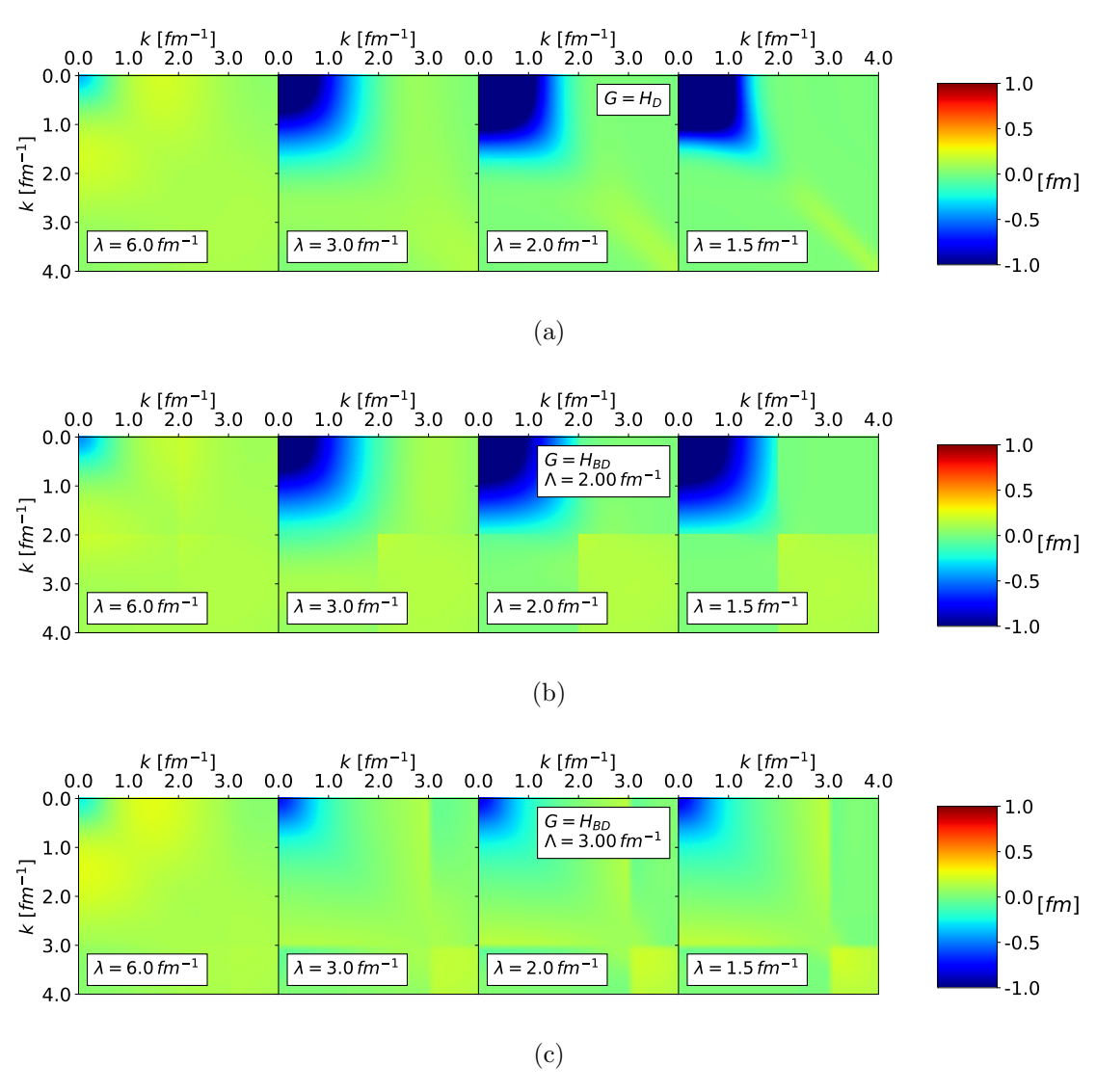


FIG. 15: Caption.

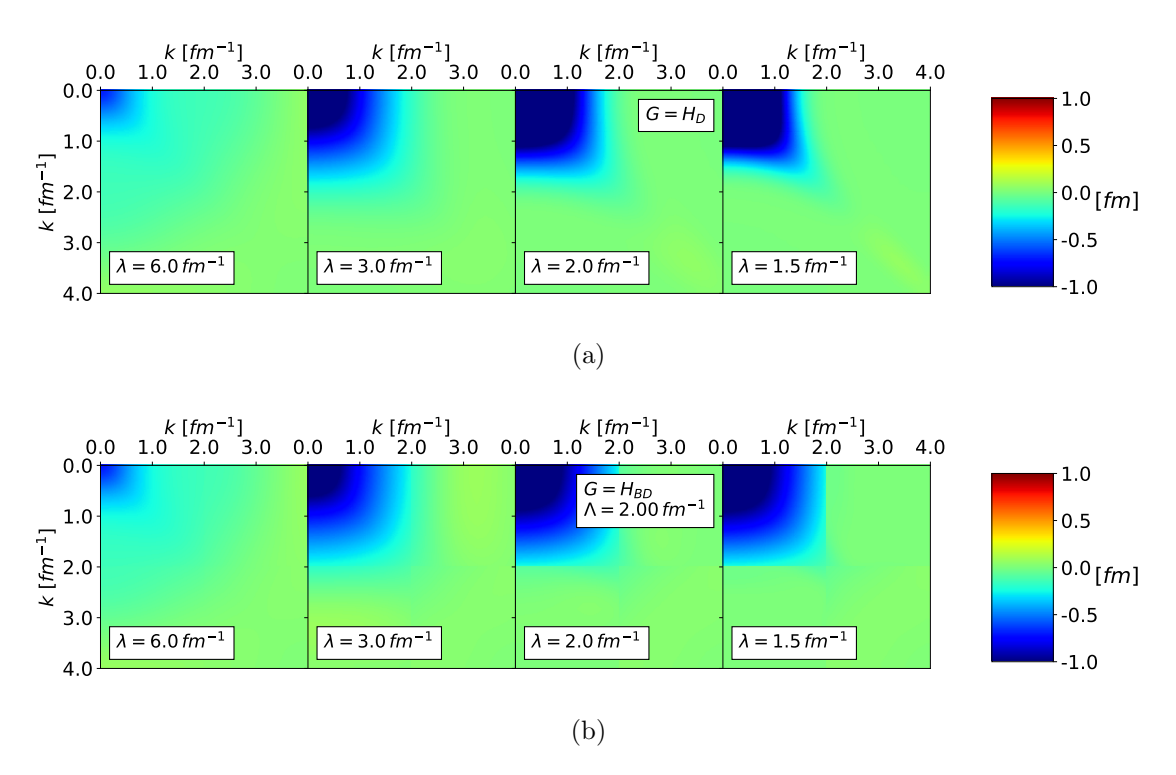


FIG. 16: Caption.

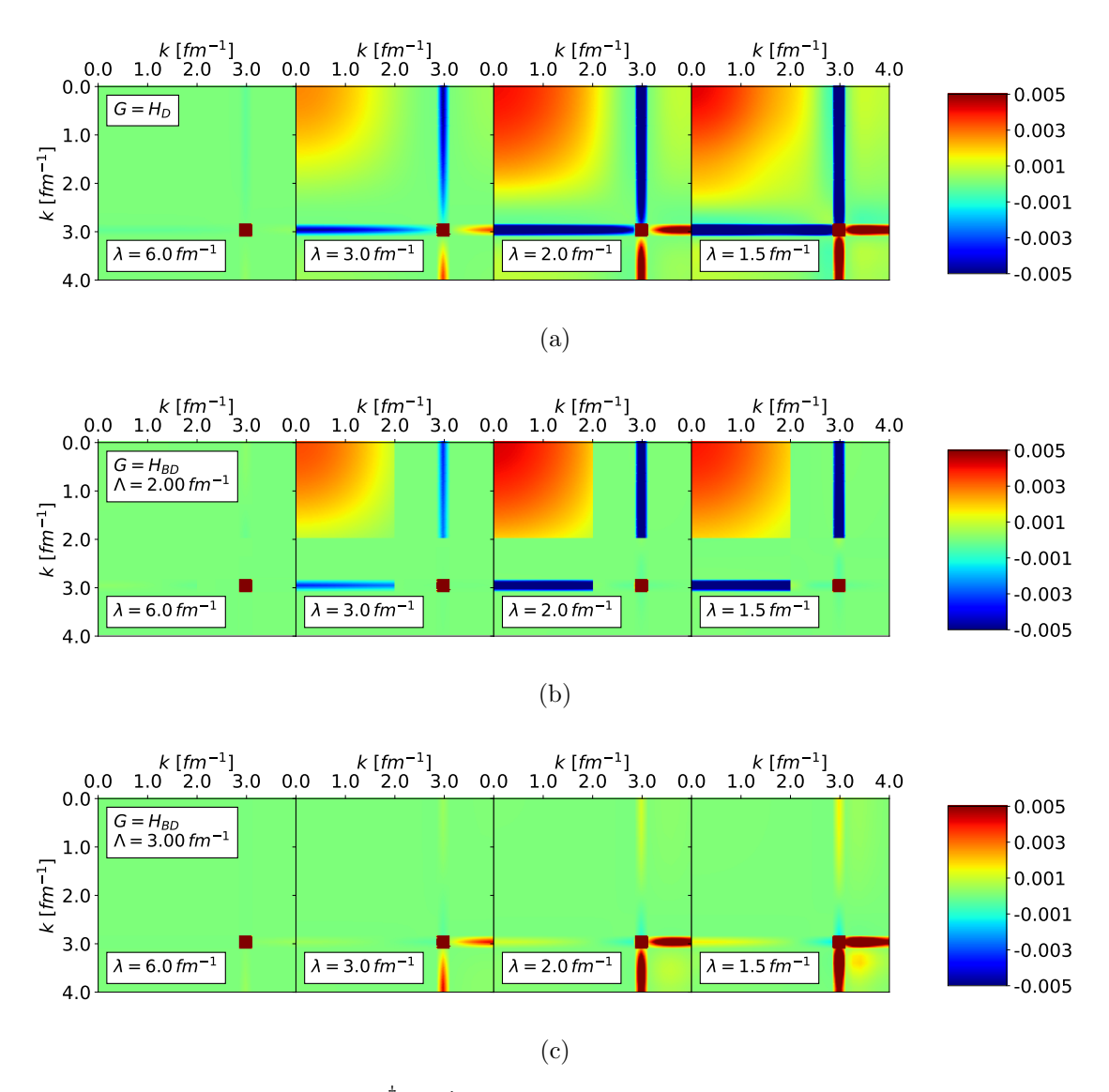


FIG. 17: Matrix elements of $\langle k|a_q^{\dagger}a_q|k'\rangle$ SRG-evolving in λ right to left under transformations from the Gezerlis et al. N²LO local potential with the Wegner generator (a) and block-diagonal generators decoupling at $\Lambda=2$ and 3 fm⁻¹ (b and c). Here q=3 fm⁻¹ and the EFT cutoff is 1 fm.

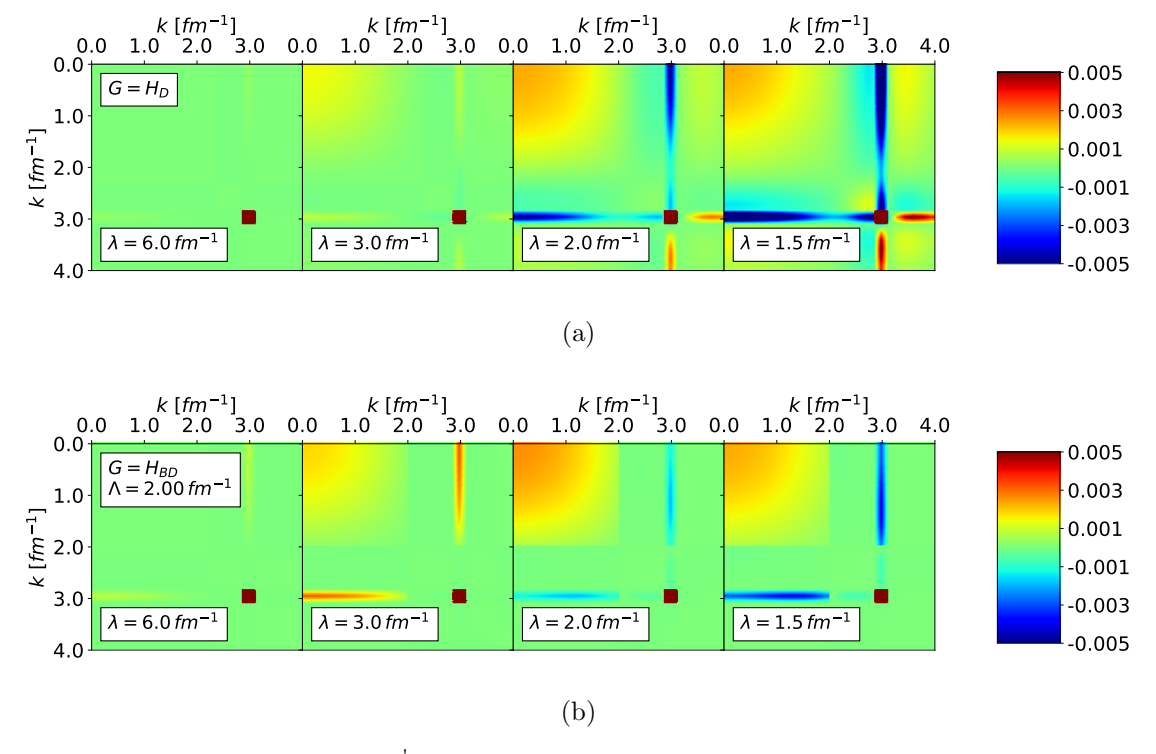


FIG. 18: Matrix elements of $\langle k|a_q^{\dagger}a_q|k'\rangle$ SRG-evolving in λ right to left under transformations from the Gezerlis et al. N²LO local potential with the Wegner generator (a) and block-diagonal generator decoupling at $\Lambda=2~{\rm fm}^{-1}$ (b). Here $q=3~{\rm fm}^{-1}$ and the EFT cutoff is 1.2 fm.

[1] D. R. Entem and R. Machleidt, Phys. Rev. C $\mathbf{68}$, 041001 (2003), arXiv:nucl-th/0304018 [nucl-th].

[2] E. R. Anderson, S. K. Bogner, R. J. Furnstahl, and R. J. Perry, Phys. Rev. C 82, 054001 (2010), arXiv:1008.1569 [nucl-th].

[3] P. Reinert, H. Krebs, and E. Epelbaum, Eur. Phys. J. A 54, 86 (2018), arXiv:1711.08821 [nucl-th].

[4] A. Gezerlis, I. Tews, E. Epelbaum, M. Freunek, S. Gandolfi, K. Hebeler, A. Nogga, and A. Schwenk, Phys. Rev. C 90, 054323 (2014), arXiv:1406.0454 [nucl-th].